Articles

Phosphine- and Pyridine-Functionalized N-Heterocyclic Carbene Methyl and Allyl Complexes of Palladium. Unexpected Regiospecificity of the Protonation Reaction of the Dimethyl Complexes

Andreas A. Danopoulos,*,† Nikolaos Tsoureas,† Stuart A. Macgregor,*,‡ and Christopher Smith‡

School of Chemistry, University of Southampton, Highfield, Southampton, U.K. SO17 1BJ, and School of Engineering and Physical Sciences, William Perkin Building, Heriot-Watt University, Edinburgh, EH14 4AS, U.K.

Received September 14, 2006

Square planar neutral dimethyl and cationic allyl complexes of palladium with the electronically nonsymmetric diphenylphosphinomethyl- and pyridyl-N-heterocyclic carbene ligands have been synthesized and characterized. The products from the protonation of the dimethyl complexes with 1 equiv of acid at low temperatures are monomethyl cations, the exact nature of which is dependent on the type of ligand; in pyridine−carbene complexes the Pd−Me bond cleaved is *trans* to the carbene, while for the phosphino−carbene complexes it is *trans* to the phosphine. Density functional calculations suggest that protonation in these complexes occurs directly at the methyl ligands and that the site of protonation determines the selectivity of Pd−Me cleavage. For the pyridine−carbene complexes there is a clear preference for protonation *trans* to the carbene. For phosphino−carbene complexes, however, the site of protonation depends on the steric bulk of the N-heterocyclic carbene ligand. Protonation *trans* to carbene is favored with small substituents (H, Me), but the bulky 2,6-$Pr^i_2C_6H_3$ susbstituent induces protonation *trans* to the phosphine, as is seen experimentally.

Introduction

The study of N-heterocyclic carbene (NHC) ligands tethered to a classical heteroatom donor via an organic linker of variable length and rigidity has attracted intense interest.[1] These ligands of various architectures and denticities[2] provide opportunities for the design of new homogeneous catalysts and the study of elementary organometallic reactions in precisely tailored electronic and steric environments. The NHC ligand forming strong $M-C_{NHC}$ bonds was originally introduced in order to circumvent problems of lability and ligand decomposition associated with the electronically similar and ubiquitous phosphines.[3] However, NHC ligands also exhibit unusual reactivity (insertion, reductive elimination, substitution),[4] which must be well understood for successful catalyst design. The coordinated NHC should affect spectroscopic and chemical behavior of other co-ligands. For example, due to their strong σ-donation (comparable to that of the trialkyphosphines),[5] the NHCs should exert a strong *trans* influence (and *trans* effect) weakening the M−L bonds *trans* to them. Although this view has been explicitly spelled out in the literature,[6] it has not been studied in detail.

We have recently reported[7] the use of the diphenylphosphino-functionalized NHC ligand 3-aryl-1-[β-(diphenylphosphino)-ethyl]imidazol-2-ylidene (C∼P) (aryl = DiPP, 2,6-$Pr^i_2C_6H_3$; Mes, 2,4,6-trimethylphenyl) for the preparation of a range of Pd(II) dimethyl complexes of the type (κ^2-C∼P)Pd$(CH_3)_2$. We have found that their protonation with 1 equiv of Brönsted acids

* Corresponding authors. E-mail: ad1@soton.ac.uk; s.a.macgregor@hw.ac.uk.

† University of Southampton.

‡ Heriot-Watt University.

(1) (a) Herrmann, W. A. *Angew. Chem., Int. Ed.* **2002**, *41*, 1290. (b) Bourisou, D.; Guerret, O.; Gabbai, F. P; Bertrand, G. *Chem. Rev.* **2000**, *100*, 39.

(2) See for example: (a) Herrmann, W. A.; Köcher, C.; Goossen, L. J.; Artus, G. R. J. *Chem.−Eur. J.* **1996**, *2*, 1627. (b) Danopoulos, A. A.; Motherwell, W. B.; Winston, S. *Chem. Commun.* **2002**, 1376. (c) Frankel, R.; Kniczek, J.; Ponikwar, W.; Noth, H.; Polborn, K.; Fehlhammer, W. P. *Inorg. Chim. Acta* **2001**, *312*, 23. (d) Hu, X.; Castro-Rodriguez, I.; Meyer, K. *J. Am. Chem. Soc.* **2004**, *126*, 13464.

(3) van Leeuwen, P. W. *Homogeneous Catalysis. Understanding the Art*; Kluwer Academic Publishers: Dortrecht, 2004; p 295.

(4) (a) McGuinness, D. S.; Saendig, N.; Yates, B. F.; Cavell, K. J. *J. Am. Chem. Soc.* **2001**, *123*, 4029. (b) McGuiness, D. S.; Cavell, K. J.; Yates, B. F.; Skelton, B. W.; White, A. H. *J. Am. Chem. Soc.* **2001**, *123*, 8317. (c) Gründemann, S.; Albrecht, M.; Kovacevic, A.; Faller, J. W.; Crabtree, R. H. *J. Chem. Soc., Dalton Trans.* **2002**, 2163. (d) Danopoulos, A. A.; Tsoureas, N.; Green, J. C.; Hursthouse, M. B. *Chem. Commun.* **2003**, 756. (e) Clement, N. D.; Cavell, K. J.; Jones, C.; Elsevier, C. *Angew. Chem., Int. Ed.* **2004**, *43*, 1277. (f) Dorta, R.; Stevens, E. D.; Nolan, S. P. *J. Am. Chem. Soc.* **2004**, *126*, 5054. (g) Gründemann, S.; Kovacevic, A.; Albrecht, M.; Faller, J. W.; Crabtree, R. H. *J. Am. Chem. Soc.* **2002**, *124*, 10473. (f) Galan, B. R.; Gembicky, M.; Dominiak, P. M.; Jerome, B.; Keister, J. B.; Diver, S. T. *J. Am. Chem. Soc.* **2005**, *127*, 15702.

(5) (a) Green, J. C.; Scurr, R. G.; Arnold, P. L.; Cloke, F. G. N. *Chem. Commun.* **1997**, 1963. (b) Green, J. C.; Herbert, B. J. *Dalton Trans.* **2005**, 1214.

(6) Gründemann, S.; Albrecht, M.; Loch, J. A.; Faller, J. W.; Crabtree, R. H. *Organometallics* **2001**, *20*, 5485.

(7) Tsoureas, N.; Danopoulos, A. A.; Tulloch, A. A. D.; Light, M. E. *Organometallics* **2003**, *22*, 4750.

10.1021/om0608408 CCC: $37.00
Publication on Web 12/07/2006

Scheme 1. Synthesis of Neutral Palladium Dimethyl Complexes[a]

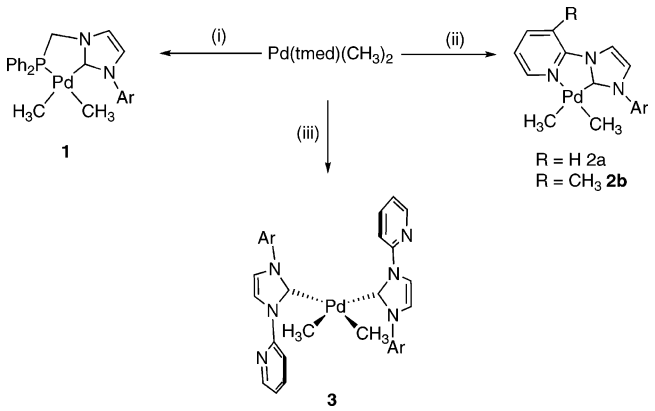

[a] Complexes in bold numbers have been structurally characterized. Ar = 2,6-diisopropylphenyl. Reagents and conditions: (i) 1 equiv [(C∧P)H]Br, 1.1 equiv $KN(SiMe_3)_2$, THF, −78 °C, then 1 equiv $Pd(tmeda)Me_2$, THF, −78 °C to RT. (ii) 1.4 equiv (C−N) (R = H), 1 equiv (C−N)* (R = Me), THF, −78 °C to RT. (iii) 2 equiv (C−N), THF, RT.

having noncoordinating anions at low temperatures in organic noncoordinating solvents, followed by trapping of the organometallic intermediate with a ligand L (L = pyridine, CH_3CN, PMe_3, etc.), proceeds with high regioselectivity, leading to the formal substitution by L of the methyl *trans* to the P atom and not *trans* to the NHC as expected.

In this paper we report (i) the use of the new, smaller bite angle ligand 3-DiPP-1-[(diphenylphosphino)methyl]imidazol-2-ylidene (C∧P) for the synthesis of the analogous complex (κ^2-C∧P)$Pd(CH_3)_2$, (ii) the use of the 3-DiPP-1-(2-pyridyl)-imidazol-2-ylidene (C−N) and 3-DiPP-1-(2-(3-methyl)pyridylimidazol-2-ylidene (C−N*) for the synthesis of complexes of type (κ^2-C−N)$Pd(CH_3)_2$ and (κ^2-C−N*)$Pd(CH_3)_2$; (iii) the preparation of cationic methallyl complexes of the type [(C∼P)Pd(methallyl)]$^+$ and [(κ^2-C−N)Pd(methallyl)]$^+$; (iv) the regioselective protonation of the new dimethyl complexes with Brönsted acids having noncoordinating anions; and (iv) attempts to rationalize the regiospecificity of the protonation reaction with the aid of density functional calculations.

All new complexes and the chemical transformations leading to them are summarized in Schemes 1−3.

Results and Discussion

Synthesis of the Neutral Dimethyl Complexes. The synthesis of the new complex (κ^2-C∧P)$Pd(CH_3)_2$, **1**, was carried out as before,[7] i.e., by reacting $Pd(tmed)(CH_3)_2$ with the phosphine-functionalized N-heterocyclic carbene (C∧P) generated *in situ* from the imidazolium salt and $KN(SiMe_3)_2$ in THF. The new complex was isolated as a yellow, air-stable powder in good yields. It was characterized by analytical and spectroscopic methods. The $^{31}P\{^1H\}$ NMR consists of a singlet at 32.7 ppm [cf. 12.45 and 12.24 for the analogous (C∼P) complexes].[7]

Scheme 3. Synthesis of Cationic Palladium Methyl Complexes[a]

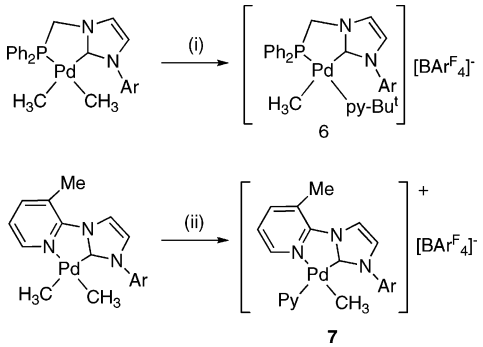

[a] Complex in bold number has been structurally characterized. Ar = 2,6-diisopropylphenyl. (i) 1 equiv $[H(OEt_2)_2]^+[BAr^F{}_4]^-$, CH_2Cl_2, −78 °C to −40 °C, then 1.1 equiv 4-Bu^{t}pyridine, −40 °C to RT; (ii) 1 equiv $[H(OEt_2)_2]^+[BAr^F{}_4]^-$, CH_2Cl_2, −78 to −40 °C, then 1.1 equiv pyridine, −40 °C to RT.

The inequivalent Pd-methyls appear as doublets ($^3J_{PH}$ = 8.1 Hz, $^3J_{PH}$ = 8.2 Hz) almost isochronous to the methyls of Pd(tmed)$(CH_3)_2$[8] but more shielded relative to *cis*-$Pd(P)_2(CH_3)_2$[9] (P = tertiary phosphine) and $[(NHC)_2{-}CH_2]Pd(CH_3)_2$.[10] The low molecular symmetry of **1** was also manifested by the appearance of the Pr^i groups of DiPP as two doublets. This observation supports a nonplanar five-membered chelate ring. The carbene NHC carbon is found at δ 190.4. The structure of **1** was determined crystallographically and is in agreement with the spectroscopic data (Figure 1).

As expected, the Pd adopts a square planar coordination geometry with a bidentate C∧P ligand. The five-membered chelate ring is puckered, and the ligand bite angle is 80.39(14)°.

Scheme 2. Synthesis of Cationic Methallyl Palladium Complexes[a]

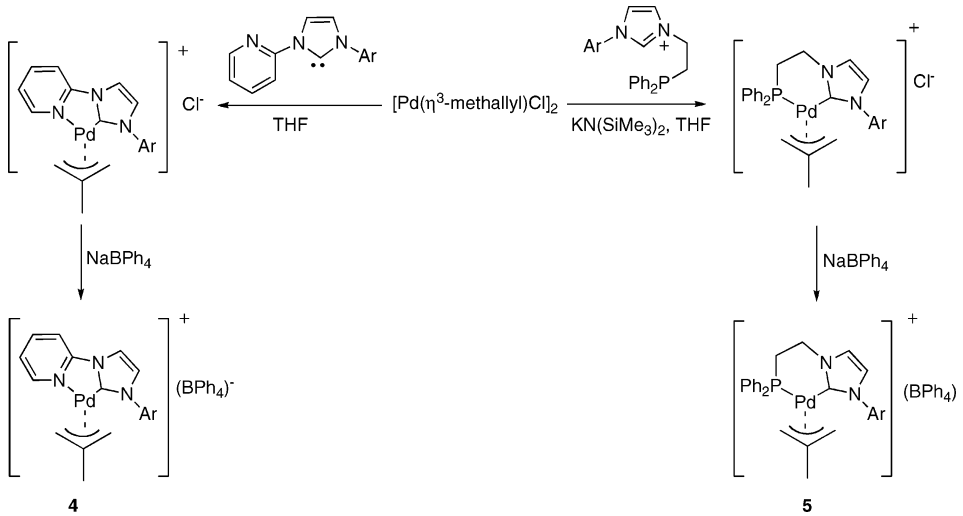

[a] Complexes in bold numbers have been structurally characterized. Ar = 2,6-diisopropylphenyl.

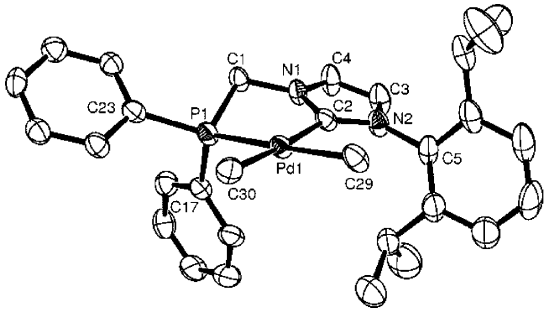

Figure 1. ORTEP representation of the structure of **1** showing 50% probability ellipsoids. H atoms are omitted for clarity. Selected bond lengths (Å) and angles (deg) with estimated standard deviations: C(2)−Pd(1) = 2.068(5), P(1)−Pd(1) = 2.293(3), C(30)−Pd(1) = 2.067(5), C(29)−Pd(1) = 2.090(5); C(2)−Pd(1)−P(1) = 80.39(14), C(30)−Pd(1)−P(1) = 98.61(14), C(29)−Pd(1)−P(1) = 176.56(14), C(2)−Pd(1)−C(29) = 96.17(19), C(30)−Pd(1)−C(2) = 176.0(2), C(30)−Pd(1)−C(29) = 84.82(19).

The Pd−CH_3 [*trans* to the NHC, 2.067(5) Å, *trans* to the phosphine, 2.090(5) Å] and the Pd−C(NHC) [2.068(5) Å] distances are all equal within the observed esd's. The interplanar angle between the heterocyclic ring plane and the coordination plane is 23.5°.

In order to gain a better insight into the structures and reactivity of the palladium *cis*-dimethyl complexes supported by heterobifunctional NHC ligands, we prepared the Pd(κ^2-C−N)$(CH_3)_2$ and Pd(κ^2-C−N*)$(CH_3)_2$ complexes, **2a** and **2b**, respectively, by the reaction of the isolated (C−N) or (C−N*)[11] with Pd(tmed)$(CH_3)_2$. *cis*-Pd(κ^2-C−N*)$(CH_3)_2$, **2b**, was obtained in good yields, by careful addition of the ligand to a cold (−78 °C) solution of the organometallic precursor, followed by slow warming; the same procedure was applied for the synthesis of **2a**, but the isolated yields were lower. Mixtures of **2a** and *cis*-Pd(κ^1-C−N)$_2(CH_3)_2$, **3**, were obtained when an excess of the ligand was used and/or by mixing the reagents at room temperature. Optimized conditions for the selective preparation of **2a** and **3** are given in the Experimental Section. The complexes **2a**, **2b**, and **3** were characterized by analytical and spectroscopic methods. The low symmetry in **2a** and **2b** is manifested by the presence of a pair of two inequivalent Pd−CH_3 resonances at δ 0.12 and 0.01 (for **2a**) and 0.22 and 0.12 (for **2b**), respectively; the downfield peaks were assigned by NOESY experiments to the methyls *trans* to the NHC groups. Compared to the corresponding methyls of the (κ^2-C∼P)Pd-$(CH_3)_2$ and (κ^2-C∧P)Pd$(CH_3)_2$, the methyls of **2a** and **2b** are deshielded. The ^{1}H NMR of **3** implies a C_2 symmetric structure (one singlet for the Pd−CH_3, four doublets and two septets for the *o*-$(CH_3)_2$CH of DiPP). The C_{NHC} was observed only for **3** at 200.1 ppm.

The structures of **2b** and **3** were confirmed crystallographically and are shown in Figures 2 and 3, respectively.

Even though the quality of the data obtained for **2b** is not suitable for the estimation of bond lengths and angles at the desired accuracy, they establish unambiguously the connectivity in the complex and allow the extraction of trends in the metrical data. The geometry around the metal center is square planar, with the (C−N*) ligand occupying two *cis* positions. The ligand

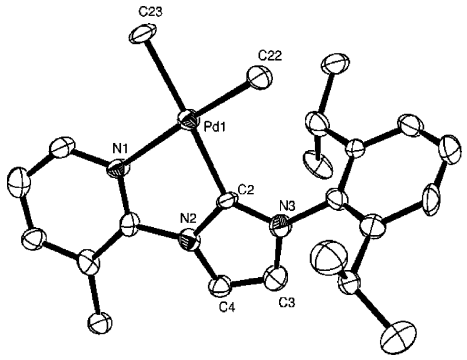

Figure 2. ORTEP representation of the structure of **2b** showing 50% probability ellipsoids. H atoms are omitted for clarity. Selected bond lengths (Å) and angles (deg): C(2)−Pd(1) = 2.038, N(1)−Pd(1) = 2.130, C(22)−Pd(1) = 2.017, C(23)−Pd(1) = 2.082; C(22)−Pd(1)−C(2) = 100.7, C(22)−Pd(1)−C(23) = 85.1, C(2)−Pd(1)−C(23) = 172.2, C(22)−Pd(1)−N(1) = 174.5, C(2)−Pd(1)−N(1) = 76.8, C(23)−Pd(1)−N(1) = 97.8.

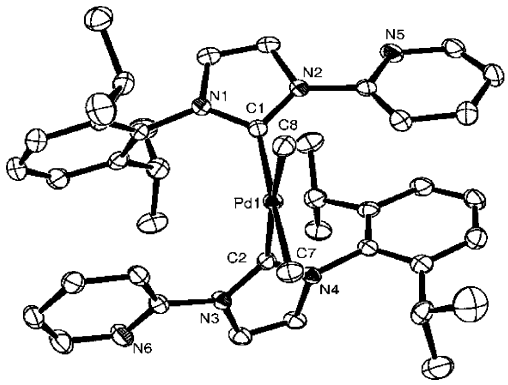

Figure 3. ORTEP representation of the structure of **3** showing 50% probability ellipsoids. H atoms are omitted for clarity. Selected bond lengths (Å) and angles (deg) with estimated standard deviations: C(1)−Pd(1) = 2.058(3), C(2)−Pd(1) = 2.064(5), Pd-(1)−C(7) = 2.101(1), Pd(1)−C(8) = 2.103(5); C(8)−Pd(1)−C(2) = 170.87(11), C(7)−Pd(1)−C(1) = 171.08, C(1)−Pd(1)−C(8) = 87.96(15), C(2)−Pd(1)−C(7) = 87.73(17), C(1)−Pd(1)−C(2) = 101.16(16).

adopts an almost coplanar conformation with the pyridine plane slightly tilted, in order to accommodate the steric requirements of the methyl substituent of the pyridine heterocycle. The ligand bite angle of 76.8° is smaller than the ones observed for complexes (κ^2-C∼P)Pd$(CH_3)_2$[7] and **1**.

Complex **3** adopts a C_2 symmetrical conformation, with the geometry around the metal center being square planar. The C_2 rotation axis lies on the coordination plane and bisects the Me−Pd−Me angle. The Pd−C_{NHC} bond distances are equal to and in the same range (within esd's) as the ones observed for the bidenate complexes **1** and **2b**. The same trend is also observed for the Pd−CH_3 bond lengths. The planes of the carbene moieties form a dihedral angle of approximately 75.5° with the coordination plane. The C_2 conformation is possibly adopted due to steric reasons, a fact that is also supported by the large C(1)−Pd(1)−C(2) angle [101.16(16)°].

Synthesis of the Cationic Methallyl Complexes. Heterobifunctional bidentate co-ligands have been used on Pd allyl complexes in order to promote selective allyl substitution at one end of the coordinated allyl.[12] The directing effect is believed to be the electronic differentiation due to the donors

(8) de Graaf, W.; Boersma, J.; Smeets, W. J. J.; Spek, A. L.; van Koten, G. *Organometallics* **1989**, *8*, 2907.
(9) Tooze, R. P.; Chiu, K. W.; Wilkinson, G. *Polyhedron* **1984**, *3*, 1025.
(10) Douthwaite, R. E.; Green, M. L. H.; Silcock, P. J.; Gomes, P. T. *J. Chem. Soc., Dalton Trans*. **2002**, 1386.
(11) Winston, S.; Stylianides, N.; Tulloch, A. A. D.; Wright, J. A.; Danopoulos, A. A. *Polyhedron* **2004**, *23*, 2813.
(12) Heumann, A. In *Transition Metals for Organc Synthesis*; Beller, M., Bolm, C., Eds.; Wiley-VCH: Weinheim, 2004; Vol. 1, p 307.

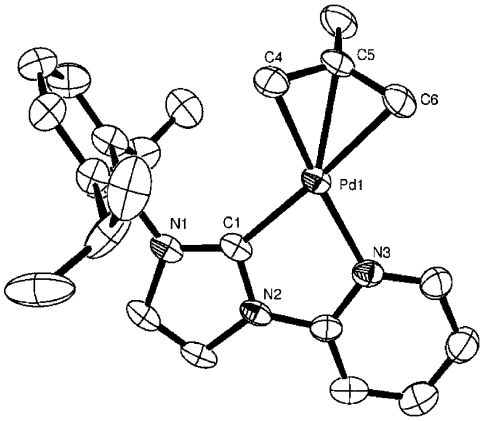

Figure 4. ORTEP representation of the cation in **4** showing 50% probability ellipsoids. H atoms and one molecule of ether are omitted for clarity. Selected bond lengths (Å) and angles (deg) with estimated standard deviations: C(2)−Pd(1) = 2.014(3), C(21)−Pd(1) = 2.165(4), C(22)−Pd(1) = 2.160(4), C(23)−Pd(1) = 2.096(5), N(1)−Pd(1) = 2.113(4); C(2)−Pd(1)−C(23) = 106.53(18), C(2)−Pd(1)−N(1) = 78.44(16), C(23)−Pd(1)−N(1) = 173.28(15), C(2)−Pd(1)−C(22) = 139.74(18) C(23)−Pd(1)−C(22) = 38.73(17), N(1)−Pd(1)−C(22) = 138.40(15), C(2)−Pd(1)−C(21) = 172.87-(18), C(23)−Pd(1)−C(21) = 68.06(18), N(1)−Pd(1)−C(21) = 106.59(16), C(22)−Pd(1)−C(21) = 37.66(17), C(21)−C(22)−C(23) = 116.3(4), C(21)−C(22)−C(24) = 120.2(4), C(23)−C(22)−C(24) = 121.8(4).

of the electronically nonsymmetric bidentate ligand. [Pd(NHC)-(allyl)Cl] complexes with monodenate NHCs have been reported and used for the generation of reactive "monoligated" [Pd(0)-(NHC)] centers.[13] In order to probe the electronic differentiation exerted by the phosphine- and pyridine-functionalized NHC ligands described above on the allyl group coordinated on Pd, we undertook the synthesis of the complexes [Pd(C−N)-(methallyl)]$^+$ and [Pd(C∼P)(methallyl)]$^+$. Complexes [Pd(C−N)(methallyl)](BPh$_4$), **4**, and [Pd(C∼P)(methallyl)](BPh$_4$), **5**, were prepared by the reaction of [Pd(methallyl)Cl]$_2$ with (C−N) or (C∼P). The crude [Pd(C−N)(methallyl)]Cl and [Pd-(C∼P)(methallyl)]Cl, which were not isolated, were transformed to **4** and **5** by anion exchange with NaBPh$_4$. The NMR spectra of the new products manifested the lack of any symmetry element in the cations and evidenced the presence of one isomer in solution. The Pr^i of the DiPP groups as well as the diastereotopic protons of the termini of the methallyl group appear as multiplets. We could not observe the C_{NHC} signal in the $^{13}C\{^1H\}$ NMR spectra in any of these complexes. The structures of **4** and **5** were confirmed crystallographically and are shown in Figures 4 and 5.

Both **4** and **5** feature bidentate (C−N) and (P∼C) ligands, the former adopting a virtually planar conformation (excluding the DiPP substituent), while in the latter the conformation of the six-membered chelate ring is best described as half-chair. The Pd−C_{NHC} bonds in **4** and **5** are similar (within the measured esd's) to the corresponding bond lengths in **1** and **2**. The bonding of the methallyl group to the metal in both complexes is nonsymmetrical, with significantly different Pd−C bonds. In **4** the Pd−C allyl carbon that is *trans* to the C_{NHC} is 2.165(4) Å, and the one *trans* to the pyridine is 2.096(5) Å. In **5** the Pd−C allyl carbon that is *trans* to the C_{NHC} is 2.154(4) Å, and the one *trans* to the P donor is 2.168(5) Å. The Pd−C (central allyl carbon) is 2.160(4) Å in **4** and 2.202(5) Å in **5**. The trends in the magnitute of these Pd−C bond lengths are analogous to those observed with the neutral dimethyl complexes described previously and may be related to differences in the *trans* influences of donor groups of the bidentate ligand. The allyl plane forms an angle of ca. 54.6° (in **4**) and ca. 53.5° (in **5**) with the coordination plane.

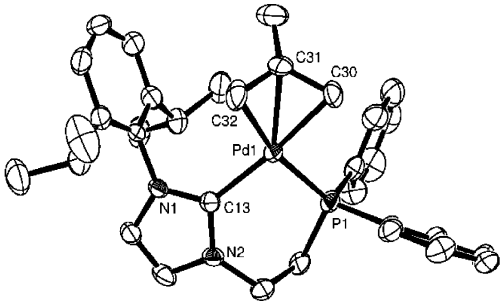

Figure 5. ORTEP representation of the cation in **5** showing 50% probability ellipsoids. H atoms are omitted for clarity. Selected bond lengths (Å) and angles (deg) with estimated standard deviations: C(13)−Pd(1) = 2.039(5); P(1)−Pd(1) = 2.2825(14); C(30)−Pd-(1) = 2.157(5); C(31)−Pd(1) = 2.202(5); C(32)−Pd(1) = 2.164(6); C(13)−Pd(1)−P(1) = 92.56(14); C(13)−Pd(1)−C(30) 168.0(2).

Protonation of the Complexes. The reaction of the complexes (κ^2-C∼P)Pd(CH$_3$)$_2$ with 1 equiv of acids H$^+$A$^-$, A$^-$ = noncoordinating anion, at low temperatures, followed by trapping of the organometallic intermediate with L (L = py, PMe$_3$, MeCN, etc.), has already been reported.[7] The unexpected regioselectivity of the reaction (100% substitution of the methyl that is *trans* to the phosphine) prompted us to explore it in detail with the other related Pd complexes that were described in the previous section.

The reaction of **1** with 1 equiv of (CF$_3$)$_2$CHOH or [H(Et$_2$O)]$^+$[BAr$^F_4$]$^-$ in CH$_2$Cl$_2$ or CH$_2$Cl$_2$/ether at −78 °C, followed by addition of 1 equiv of 4-Bu^t-pyridine at −40 °C and warming to room temperature, gave on workup a white, air-stable solid, **6**. The appearance of one Pd−CH$_3$ peak in the ^{1}H NMR spectrum (δ 0.04, broad singlet) in addition to resonances due to pyridine, the (C∧P) ligand, and the anion, and one signal in the $^{31}P\{^1H\}$NMR spectrum (δ 55.3), deshielded relative to **1**, support the presence of one isomer in solution. Even though crystals of this complex suitable for X-ray diffraction could not be grown, the proposed structure (Scheme 3) in which the Bu^t-pyridine is *trans* to the phosphine is based on comparison of the NMR data with the already structurally characterized [(κ^2-C∼P)Pd(CH$_3$)(py)]$^+$ analogue.[7] It is interesting to notice that monitoring the reaction by ^{1}H NMR spectroscopy at low temperatures confirmed that a single species was formed at lower temperatures exhibiting the same spectrum as the isolated complex, eliminating the possibility of isomerization in solution prior to the isolation of **6**.

Analogous reaction of **2b** with 1 equiv of [H(Et$_2$O)]$^+$[BAr$^F_4$]$^-$ followed by addition of pyridine gave the cationic complex **7** as a single isomer, which was characterized analytically, spectroscopically, and crystallographically. In the ^{1}H NMR spectrum, the single Pd−CH$_3$ resonance (δ −0.09) of the cationic **7** is shielded relative to **2b**. The configuration of **7** in solution was established by NOESY NMR spectroscopy and showed that substitution *trans* to the NHC donor has taken place. Monitoring the reaction at lower temperatures (−40 °C) by ^{1}H NMR shows that the product formed originally at lower temperatures was identical to that of the isolated **7**. The structure of **7** was determined crystallographically and is in agreement with the spectroscopic assignments (Figure 6).

The geometry around the Pd center is square planar, with the pyridine ligand being *trans* to the NHC and the remaining

(13) Marion, N.; Navarro, O.; Mei, J.; Stevens, E. D.; Scott N. M.; Nolan, S. P. *J. Am. Chem. Soc.* **2006**, *128*, 4101.

Table 1. Crystallographic Data for the Compounds Described in the Paper

	1	**2b**	**3**	**4**	**5**	**7**
chemical formula	$C_{30}H_{37}N_2PPd$	$C_{23}H_{31}N_3Pd$	$C_{42}H_{52}N_6Pd$	$C_{48}H_{50}BN_3Pd$	$C_{57}H_{60}BN_2PPd$	$C_{59}H_{45}BF_{24}N_4Pd$
fw	562.99	455.9	747.30	786.12	921.25	1383.20
cryst syst	orthorhombic	monoclinic	monoclinic	triclinic	monoclinic	monoclinic
space group	$P2_12_12_1$	$P2_1/c$	$P2_1/n$	$P\bar{1}$	Cc	$P2_1/n$
a/Å	10.031(13)	10.408(6)	10.936(14)	13.149(2)	16.070(3)	24.5559(8)
b/Å	11.34(2)	12.139(7)	27.06(3)	14.181(2)	16.422(3)	19.7453(7)
c/Å	24.499(8)	17.357(11)	13.47(4)	15.6998(17)	19.758(4)	25.285(8)
α/deg	90	90	90	115.110(12)	90	90
β/deg	90	105.97(4)	107.64(19)	90.856(13)	112.77(3)	97.3400(10)
γ/deg	90	90	90	114.148(16)	90	90
Z	4	4	4	2	4	8
T/K	120(2)	120(2)	120(2)	120(2)	120(2)	120(2)
μ/mm^{-1}	0.743	0.892	0.526	0.425	0.458	0.420
no. of data collected	24 799	22 013	33 787	40 241	13 505	120 423
no. of unique data	6316	3714	6436	10 833	5433	27 861
goodness of fit on F^2	1.028	1.188	1.047	1.056	0.997	1.031
R_{int}	0.1060	0.1620	0.0674	0.0936	0.0648	0.1433
final $R(\|F\|)$ for $F_o > 2\sigma(F_o)$	0.0483	0.1037	0.0363	0.0680	0.0417	0.0786
final $R(F^2)$ for all data	0.0785	0.1204	0.0507	0.0989	0.0618	0.1526

Me group *trans* to the pyridine. The angle formed between the pyridine (L) plane and the coordination plane is 74.9°. The Pd−C_{NHC} and Pd−CH_3 bonds in **7** are shorter than in the corresponding $[(\kappa^2\text{-C}\sim\text{P})Pd(CH_3)(py)]^+$ previously reported,[7] while the Pd−N(pyridine) bonds in the two complexes are equal.

Computational Studies. We have employed density functional calculations to rationalize the selectivities of the protonation/substitution reactions and have focused on the $(\kappa^2\text{-C}\sim\text{P})Pd(CH_3)_2$[7] and $(\kappa^2\text{-C}-\text{N})Pd(CH_3)_2$ systems. In particular, the observation of substitution *trans* to phosphorus upon protonation of $(\kappa^2\text{-C}\sim\text{P})Pd(CH_3)_2$ was initially surprising, as the NHC arm of the C∼P ligand might have been expected to exert a higher *trans* influence and *trans* effect than the phosphine moiety.[6]

Two model systems were used in the calculations. In model 1 all ligand substituents were replaced by hydrogens, while in model 2 the full $(\kappa^2\text{-C}\sim\text{P})Pd(CH_3)_2$ and $(\kappa^2\text{-C}-\text{N})Pd(CH_3)_2$ molecules were considered. Computed Pd−ligand distances are compared with those determined crystallographically in Table 2.

Model 1 generally provides good agreement with experiment, although the Pd−N bond length is somewhat overestimated compared to the crystal data for $(\kappa^2\text{-C}-\text{N*})Pd(CH_3)_2$. In model 2 inclusion of the full ligand causes the Pd−P bond in $(\kappa^2\text{-C}\sim\text{P})Pd(CH_3)_2$ to lengthen by 0.04 Å, but otherwise the Pd−ligand bond distances are not significantly affected, suggesting minimal electronic effects arising from the ligand substituents. Of prime interest are the relative lengths of the Pd−CH_3 bonds, and for $(\kappa^2\text{-C}\sim\text{P})Pd(CH_3)_2$ the calculations find these to be slightly longer when *trans* to carbene, by 0.005 Å (model 1) and 0.013 Å (model 2). Experimentally, it is the Pd−CH_3 bond *trans* to carbene that is slightly shorter, although the difference is not significant when the experimental errors are considered. Both models of $(\kappa^2\text{-C}-\text{N})Pd(CH_3)_2$ correctly reproduce the longer Pd−CH_3 bond *trans* to carbene seen experimentally, this being longer by 0.032 Å (model 1) and 0.025 Å (model 2), although these differences are somewhat smaller than those determined experimentally.

The experimental and computed Pd−CH_3 distances provide a basis for estimating the *trans* influence of the donor atoms in the C−N and C∼P ligands. For the C−N ligand both approaches indicate that the NHC arm has the significantly higher *trans* influence. In contrast, for the C∼P ligand the *trans* influences of the NHC and the alkyldiarylphosphine moieties appear to be very similar, although the calculations do suggest a slightly higher *trans* influence for the NHC donor in the C∼P ligand.

Table 2. Computed Pd−Ligand Bond Distances (Å) in $(\kappa^2\text{-C}\sim\text{P})Pd(CH_3)_2$ and $(\kappa^2\text{-C}-\text{N*})Pd(CH_3)_2$ Species Using Model 1 and Model 2[a]

$(\kappa^2\text{-C}\sim\text{P})Pd(CH_3)_2$		Pd-C_{NHC}	Pd-P	Pd-$C_{trans\text{-}C}$	Pd-$C_{trans\text{-}P}$
	Model 1 (R = R' = H)	2.067	2.305	2.101	2.096
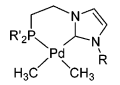	Model 2 (R = DiPP; R' = Ph)	2.080	2.345	2.107	2.094
	Experiment (R = DiPP; R' = Ph)	2.088(5)	2.2994(13)	2.098(5)	2.111(5)
$(\kappa^2\text{-C-N})Pd(CH_3)_2$		Pd-C_{NHC}	Pd-N	Pd-$C_{trans\text{-}C}$	Pd-$C_{trans\text{-}N}$
	Model 1 (R = R' = H)	2.021	2.187	2.080	2.048
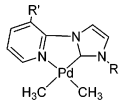	Model 2 (R = DiPP; R' =H)	2.043	2.178	2.077	2.052
	Experiment (R = DiPP; R'= Me)	2.038	2.130	2.082	2.017

[a] Corresponding distances determined crystallographically are included for comparison.

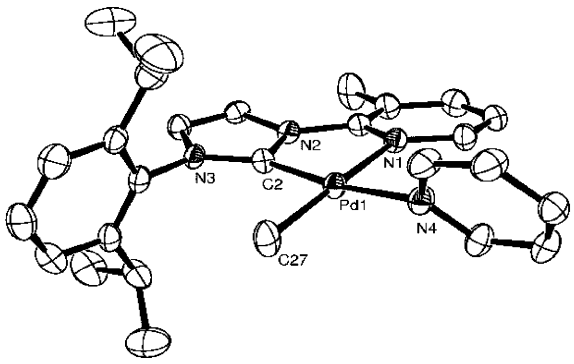

Figure 6. ORTEP representation of the structure of the cation in **7** showing 50% probability ellipsoids. The asymmetric unit consists of two cations and two anions. The $[BAr^F_4]^-$ anion and H atoms are omitted for clarity. Selected bond lengths (Å) and angles (deg) with estimated standard deviations: C(2)−Pd(1) = 1.964(5), N(4)−Pd(1) = 2.084(4), N(1)−Pd(1) = 2.154(4), C(27)−Pd(1) = 2.021(5), C(2)−Pd(1)−C(27) = 96.9(2), C(2)−Pd(1)−N(4) = 172.2(2), C(27)−Pd(1)−N(4) = 87.96(19), C(2)−Pd(1)−N(1) = 78.16(18), C(27)−Pd(1)−N(1) = 172.1(2), N(4)−Pd(1)−N(1) = 97.65(16).

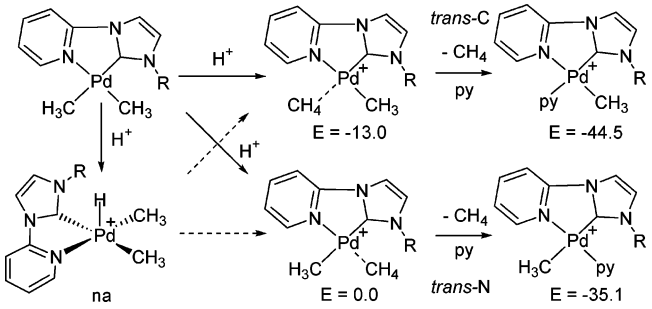

Figure 7. Key stationary points computed along the protonation/substitution reaction of (κ^2-C−N*)Pd(CH_3)$_2$, with model 1 (R = R′ = H). Energies are relative to *trans*-N [(κ^2-C−N*)Pd(CH_3)(CH_4)]$^+$ set to zero. No local minimum corresponding to [(κ^2-C−N*)Pd(CH_3)$_2$(H)]$^+$ could be located.

If this is the case, however, then it would appear to be inconsistent with the experimental observation of substitution *trans* to phosphine upon protonation.

We therefore turned to consider the protonation and subsequent CH_4/py substitution reactions, and our approach is illustrated in Figure 7 for (κ^2-C−N)Pd(CH_3)$_2$. Protonation of this species could occur at the Pd center, to give the five-coordinate intermediate [(κ^2-C−N)Pd(CH_3)$_2$(H)]$^+$. From this species C−H bond coupling would yield one of two isomers of the CH_4 σ-complex, [(κ^2-C−N)Pd(CH_3)(CH_4)]$^+$, with CH_4 *trans* to either carbene (*trans*-C) or pyridine (*trans*-N). Alternatively, protonation could occur initially at the methyl groups to form either of these two CH_4 σ-complexes directly. CH_4/py substitution would then give the *trans*-C or *trans*-N forms of the final product, [(κ^2-C−N)Pd(CH_3)(py)]$^+$. We shall first describe our results for the (κ^2-C−N)Pd(CH_3)$_2$ system for which the *trans*-C product is observed experimentally. An analogous scheme will then be considered for (κ^2-C∼P)Pd(CH_3)$_2$.

With model 1, all attempts to locate the putative five-coordinate intermediate [(κ^2-C−N)Pd(CH_3)$_2$(H)]$^+$ as a local minimum failed. An approximate geometry and energy for this species were generated by assuming a square pyramidal structure with an axial hydride and with all H−Pd−ligand angles constrained to 90°. Upon releasing these angular constraints, however, the axial hydride transferred directly onto the CH_3 ligand *trans* to carbene to form the *trans*-C CH_4 σ-complex [Pd(κ^2-C−N)(CH_3)(CH_4)]$^+$. This σ-complex was estimated to be at least 30 kcal/mol more stable than the constrained-angle structure of [Pd(κ^2-C−N)(CH_3)$_2$(H)]$^+$. Moreover, the *trans*-C form of [Pd(κ^2-C−N)(CH_3)(CH_4)]$^+$ was 13.0 kcal/mol more stable than the alternative *trans*-N isomer (see Figure 7). This preference was retained in the final product, the *trans*-C form of [(κ^2-C−N)Pd(CH_3)(py)]$^+$ being 9.4 kcal/mol more stable than the *trans*-N alternative. Thus the calculations employing model 1 indicate a strong preference for direct protonation of the methyl group *trans* to carbene, and this is consistent with the experimental observation of substitution *trans* to carbene upon protonation. This assertion assumes facile CH_4/py substitution in [Pd(κ^2-C−N)(CH_3)(CH_4)]$^+$, and this process is certainly extremely exothermic (by more than 30 kcal/mol). Subsequent calculations on the [(κ^2-C∼P)Pd(CH_3)(CH_4)]$^+$ system also indicated that the barriers associated with CH_4/py substitution in these systems should be small (see below). The relative energies of the isomers of [Pd(κ^2-C−N)(CH_3)(CH_4)]$^+$ and [(κ^2-C−N)Pd(CH_3)(py)]$^+$ both reflect the higher *trans* influence of the carbene arm of the C−N ligand, with the more stable form in each case having the more weakly bound ligand (CH_4 and py, respectively) *trans* to the carbene.

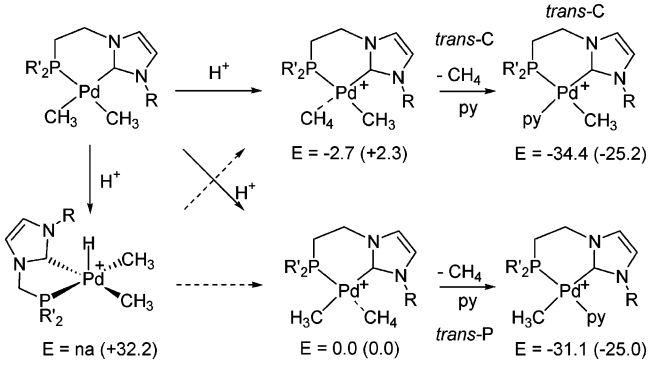

Figure 8. Relative energies (kcal/mol) of species along the protonation/substitution reaction of (κ^2-C−P)Pd(CH_3)$_2$ with model 1 (R = R′ = H) and (in parenthesis) model 2 (R = DiPP; R′ = Ph). Energies are relative to *trans*-P [(κ^2-C∼P)Pd(CH_3)(CH_4)]$^+$ set to zero. No local minimum corresponding to [(κ^2-C∼P)Pd(CH_3)$_2$(H)]$^+$ could be located with model 1.

We then considered the protonation/substitution reaction of (κ^2-C∼P)Pd(CH_3)$_2$, again initially with model 1 (see Figure 8). As with (κ^2-C−N)Pd(CH_3)$_2$ we were unable to locate a stable species resulting from direct protonation at Pd, and unconstrained hydride structures corresponding to [(κ^2-C∼P)Pd(CH_3)$_2$(H)]$^+$ all relaxed to *trans*-C [(κ^2-C∼P)Pd(CH_3)(CH_4)]$^+$. This species was found to be 2.7 kcal/mol more stable than the *trans*-P isomer, and this preference was retained in the final product, [(κ^2-C∼P)Pd(CH_3)(py)]$^+$, where the *trans*-C isomer was more stable by 3.3 kcal/mol. CH_4/py substitution is again a strongly exothermic process. Most importantly, with model 1 both the initial site of protonation and the energy of the final product indicate a small preference for reaction *trans* to the carbene arm of the C∼P ligand. This is at odds with the experimental observation of protonation/substitution *trans* to the phosphine arm of the C∼P ligand in (κ^2-C∼P)Pd(CH_3)$_2$. We therefore extended our study to include the full ligand substituents through use of model 2.

The energies of the species calculated with model 2 are included in parentheses in Figure 8. Unlike model 1, in this case we were able to locate a local minimum corresponding to [(κ^2-C∼P)Pd(CH_3)$_2$(H)]$^+$, although this remains a very high-energy structure, which is at least 30 kcal/mol above both isomers of [(κ^2-C∼P)Pd(CH_3)(CH_4)]$^+$. Direct protonation at the methyl ligands is therefore much more likely, and with model 2 the *trans*-P isomer of [(κ^2-C∼P)Pd(CH_3)(CH_4)]$^+$ in fact becomes the more favored species, being 2.3 kcal/mol more stable than the *trans*-C isomer. Upon CH_4/pyridine substitution, however, the preference swaps again and the *trans*-C product becomes more stable, albeit by only 0.3 kcal/mol. The calculations therefore suggest that the introduction of the full steric bulk of the C∼P ligand causes a switch in the preferred site of protonation, from *trans* to carbene in model 1 to *trans* to phosphine in model 2. The energy differences involved are small, however, and so to ensure that the computed preferred site of protonation does indeed equate to the same selectivity in the final observed products, we have studied the mechanism of CH_4/py substitution in both [(κ^2-C∼P)Pd(CH_3)(CH_4)]$^+$ intermediates.

The two limiting mechanisms for CH_4/py substitution in [(κ^2-C∼P)Pd(CH_3)(CH_4)]$^+$ involve either dissociative or associative displacement, and computed reaction profiles for both isomers are shown in Figure 9. Dissociation of CH_4 leads to the T-shaped 14*e* intermediates, T_C or T_P [(κ^2-C∼P)Pd(CH_3)]$^+$, of which the T_P isomer is significantly more stable by 9 kcal/mol. Moreover, we were able to locate a transition state for CH_4 loss from

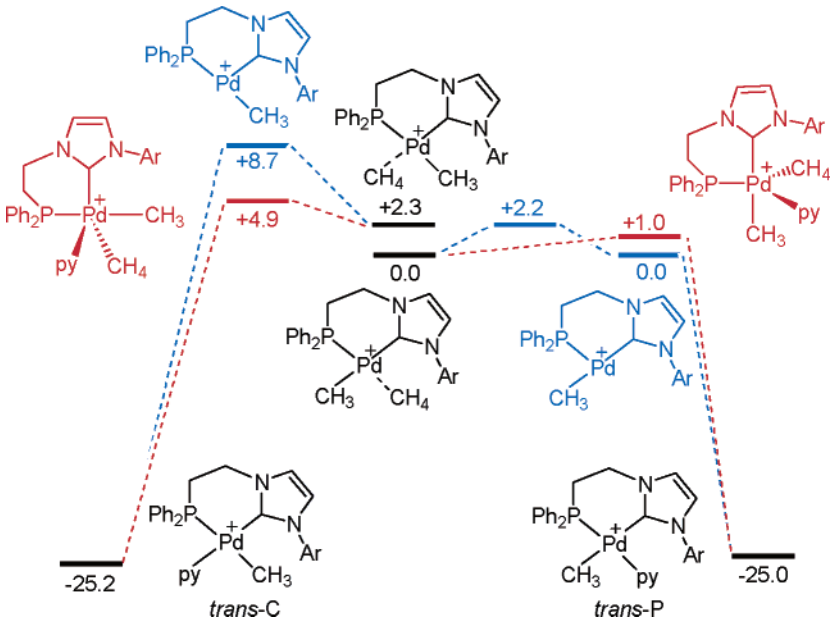

Figure 9. Computed reaction profiles (kcal/mol) for CH_4/py substitution in $[(\kappa^2\text{-C}\sim\text{P})Pd(CH_3)(CH_4)]^+$ species to give *trans*-P $[(\kappa^2\text{-C}\sim\text{P})Pd(CH_3)(py)]^+$ (right) or *trans*-C $[(\kappa^2\text{-C}\sim\text{P})Pd(CH_3)(py)]^+$ (left). Key species for dissociative (blue) and associative substitution (red) are indicated. See text for details.

trans-P $[(\kappa^2\text{-C}\sim\text{P})Pd(CH_3)(CH_4)]^+$, which corresponds to a very low activation barrier of only 2.2 kcal/mol. In contrast, a reaction profile probing CH_4 loss from *trans*-C $[(\kappa^2\text{-C}\sim\text{P})Pd(CH_3)(CH_4)]^+$ showed the energy to rise steadily to the level of the T_C 14*e* intermediate, and the energy of this species (plus free CH_4) therefore provides a lower limit for the CH_4 dissociation barrier of 6.4 kcal/mol, relative to *trans*-C $[(\kappa^2\text{-C}\sim\text{P})Pd(CH_3)(CH_4)]^+$. Overall the calculations indicate that a dissociative mechanism for CH_4/py substitution in $[(\kappa^2\text{-C}\sim\text{P})Pd(CH_3)(CH_4)]^+$ species will be more accessible from the *trans*-P rather than the *trans*-C isomer. The lower energy of the T_P form of $[(\kappa^2\text{-C}\sim\text{P})Pd(CH_3)]^+$ appears to be due to an agostic interaction between Pd and a C−H bond from one of the isopropyl substituents (Pd···H = 2.38 Å; C−H = 1.12 Å). In contrast the closest Pd···H contact in the T_C isomer is 2.67 Å (again to an isopropyl hydrogen), although in this case the C−H bond is directed toward an axial position and so is poorly oriented to participate in agostic bonding.

For the associative displacement mechanism the very large size of the $[(\kappa^2\text{-C}\sim\text{P})Pd(CH_3)(CH_4)]^+$/py system hampered the location and full characterization of transition state structures. Instead we have employed reaction profiles based on Pd···N(py) distances to estimate the barriers involved. This gives a value of 1.0 kcal/mol for CH_4/py substitution in *trans*-P $[(\kappa^2\text{-C}\sim\text{P})Pd(CH_3)(CH_4)]^+$ while the transition state is estimated to be about 4 kcal/mol higher in the *trans*-C isomer (see Supporting Information). Subsequently, we were able to locate a transition state for the *trans*-P pathway, and this corresponded to an activation barrier of 0.9 kcal/mol, in good agreement with the estimated value. As with the dissociative process modeled above, therefore, CH_4/py substitution in $[(\kappa^2\text{-C}\sim\text{P})Pd(CH_3)(CH_4)]^+$ via an associative process is also kinetically more accessible from the *trans*-P rather than the *trans*-C isomer.

The calculations on the full system using model 2 show that the preferred site of protonation at $(\kappa^2\text{-C}\sim\text{P})Pd(CH_3)_2$ is the methyl group *trans* to the phosphine arm. The site of protonation will also dictate the regioselectivity of CH_4/py substitution, as the subsequent steps in this process (by either a dissociative or an associative mechanism) have minimal activation barriers. However, of the two possibilities, CH_4/py substitution *trans* to phosphine is more accessible than that *trans* to carbene.

The key factor in determining the site of protonation appears to be the relief of steric strain that occurs upon protonation *cis* to the bulky DiPP group. With model 1—which may be considered as giving the ideal structure in the absence of steric effects—the computed structure of $(\kappa^2\text{-C}\sim\text{P})Pd(CH_3)_2$ is close to square planar with *trans*-C−Pd−P and *trans*-C−Pd−C angles of 175.3° and 178.5°, respectively, and the carbene ring is close to coplanar with the Pd coordination plane (N−C−Pd−P = 16°). With model 2, however, a more distorted geometry is seen (*trans*-C−Pd−C = 173.6°, *trans*-C−Pd−P = 167.1°) and the carbene ring is forced to rotate out of the Pd coordination plane (N−C−Pd−P = 29°). Similar distortions are maintained in the structure of *trans*-C $[(\kappa^2\text{-C}\sim\text{P})Pd(CH_3)(CH_4)]^+$ (*trans*-C−Pd−P = 168.6°; N−C−Pd−P = 37°), where DiPP is still *cis* to a rigid Pd−Me bond. In contrast, in *trans*-P $[(\kappa^2\text{-C}\sim\text{P})Pd(CH_3)(CH_4)]^+$ the *trans*-C−Pd−C angle increases to 176.9° while the carbene is able to rotate closer to the "ideal" orientation of model 1 (N−C−Pd−P = 20°, cf. 16°). This is presumably because the DiPP group is now *cis* to a more accommodating CH_4 ligand.

It follows from the above that the use of a smaller substituent on the carbene should tend to favor reaction *trans* to the carbene. We have tested this computationally by replacing the DiPP group in model 2 with Me, and as predicted, the isomers of $[(\kappa^2\text{-C}\sim\text{P})Pd(CH_3)(CH_4)]^+$ do become closer in energy, although the *trans*-P form is still slightly more stable by 0.5 kcal/mol. Unfortunately, we have been unable to test this idea experimentally, as the reaction of $Pd(tmed)(CH_3)_2$ with the analogue of C∼P having a methyl-substituted NHC donor gave mixtures of complexes that were difficult to purify, thus hampering further characterization. We were, however, able to test the link between *trans* influence and the nature of the carbene substituent by computing different models for the structure of $[(\kappa^2\text{-C}\sim\text{P})Pd(2\text{-methylallyl})]^+$ (see Table 3). For model 1, where all substituents were represented by hydrogen, the carbene moiety does exert the greater *trans* influence, with the Pd−C bond *trans* to carbene being longer by 0.025 Å. This difference is reduced to 0.017 Å upon introduction of a Me substituent on the carbene

Table 3. Computed Pd−Ligand Bond Distances (Å) in $[(\kappa^2\text{-C}\sim\text{P})\text{Pd}(\eta\text{-allyl})]^+$ Complexes[a]

$[(\kappa^2\text{-C}\sim\text{P})\text{Pd(allyl)}]^+$		Pd-C_{NHC}	Pd-P	Pd-$C_{trans\text{-}C}$	Pd-$C_{trans\text{-}P}$
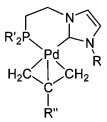	Model 1 (R = R' = R" = H)	2.045	2.318	2.223	2.198
	Model 2 (R = Me, R' = R" = H)	2.057	2.323	2.220	2.203
	Model 3 (R = DiPP; R' = Ph, R" = Me)	2.061	2.333	2.196	2.214
	Experiment	2.039(5)	2.2825(14)	2.157(5)	2.164(6)

[a] Corresponding distances determined crystallographically for **5** are included for comparison.

(model 2). The trend is reversed in the computed structure of the full molecule (model 3), with the Pd−C bond *trans* to phosphine now being longer by 0.018 Å. Thus the relative *trans* influences of the carbene and phosphine arms in these mixed C∼P ligands are clearly a function of the steric bulk of the carbene substituent.

Conclusions

The synthesis of *cis* dimethyl complexes of palladium supported by mixed donor N-heterocyclic carbene−phosphine or −pyridine bidentate ligands allowed a detailed comparative study of the ligand effects on structural and reactivity differences of the methyl co-ligands *trans* to the NHC and classical donor, respectively. The experimental data show that the N-heterocyclic carbene exerts a stronger *trans* influence than the pyridine and promotes selective substitution of the methyl *trans* to it. These findings are confirmed by density functional calculations, which show the preferred site of protonation is at the methyl group *trans* to the NHC.

In contrast, the *trans* influence of the NHC compared to the phosphine is not clear-cut experimentally due to the esd's of the crystal structure determinations. However, in this case substitution occurs selectively at the position *trans* to phosphine. The calculations suggest a slightly higher *trans* influence compared to phosphine in the NHC−phosphine ligands. However, the selectivity of protonation depends on the steric bulk of the carbene substituent: protonation is favored *trans* to the NHC for small substituents (H, Me) and swaps to *trans* to phosphine for the DiPP substituent used experimentally. Thus agreement with experiment could only be obtained once the full ligand substituents were incorporated into the computational model. The computed results suggest that the selectivity of the protonation/substitution reaction can be controlled by judicious choice of ligand substituent. Such subtle effects may arise from the unique shape of the NHC ligand and must be taken into consideration when using them as phosphine substitutes in homogeneous catalysis.

Finally, cationic Pd−allyl complexes with the same heterobifunctional bidentate ligands show Pd−C_{allyl} bond trends in agreement with the above classification of the NHC, phosphine, and pyridine donors. Computation of the Pd−C_{allyl} bond lengths shows that they are dependent on the substitution of the P and NHC donors in line with the dimethyl complexes described above.

Further work involving extensions to Pt and other transition metals and aiming at the understanding of the metal−NHC bonding in relation to observed reactivity is in progress.

Experimental Section

General Methods. Elemental analyses were carried out by the London Metropolitan University microanalytical laboratory. All manipulations were performed under nitrogen in a Braun glovebox or using standard Schlenk techniques, unless stated otherwise. Solvents were dried using standard methods and distilled under nitrogen prior use. The light petroleum used throughout had a bp of 40−60 °C.

The starting materials Pd(tmed)Me_2,[8] $[H(OEt_2)_2]^+[BAr^F{}_4]^-$,[15] and (C−N)[11] (R = H, R = Me) ligands were prepared according to literature procedures. NMR data were recorded on Bruker AV-300 and DPX-400 spectrometers, operating at 300 and 400 MHz (^{1}H), respectively. The spectra were referenced internally using the signal from the residual protiosolvent (^{1}H) or the signals of the solvent (^{13}C). ^{31}P{^{1}H} NMR spectra were recorded on a Bruker AV-300, at 121.44 MHz, and referenced externally relative to 85% H_3PO_4 in D_2O. ^{19}F NMR spectra were recorded on a Bruker AV-300, at 282.36 MHz, and were referenced externally relative to $CFCl_3$.

Synthesis of Proligand $(\text{P}\wedge\text{CH})^+\text{Br}^-$. A 3.0 g (10 mmol) amount of $Ph_2P(O)CH_2Br$[16] and 3.5 g (15 mmol) of 3-DiPP-imidazole were charged in an ampule, which was sealed under vacuum. The ampule and its contents were heated at 140 °C for one week in a thermostated oil bath. After the completion of the reaction, the contents of the ampule were dissolved in dichloromethane. Removal of the volatiles under reduced pressure produced a brown, sticky solid. This was redissolved in the minimum amount of dichloromethane and precipitated by addition of a 4:1 (v/v) mixture of ether/petroleum ether. The hygroscopic solid was immediately filtered and washed with ether (3 × 60 mL). It can be further purified by dissolving in the minimum amount of THF and precipitating with ether. The white solid thus isolated was pure for the next step. Crystalline material was obtained by cooling the filtrate of the last precipitation at 5 °C. ^{1}H NMR δ ($CDCl_3$): 1.01 [6H, d, $^3J_{HH}$ = 6.8 Hz, $CH(CH_3)_2$], 1.12 [6H, d, $^3J_{HH}$ = 6.8 Hz, $CH(CH_3)_2$], 1.94 [2H, septet, $^3J_{HH}$ = 6.8 Hz, $CH(CH_3)_2$], 6.25 [2H, d, $^2J_{PH}$ = 6.6 Hz, $Ph_2P(O)CH_2$−imidazolium], 6.99 (1H, dd, J_{HH} = 1.7 Hz, J_{HH} = 1.9 Hz, imidazole backbone), 7.21 (2H, d, $^3J_{HH}$ = 7.7 Hz, aromatic), 7.32 (1H, br s, imidazole backbone), 7.50 (1H, t, $^3J_{HH}$ = 7.7 Hz, aromatic), 7.55−7.63 (6H, m, aromatic), 8.22−8.31 (5H, m, aromatic), 10.2 (1H, br d, J_{HH} = 1.13 Hz, NCHN). ^{13}C{^{1}H} NMR δ ($CDCl_3$): 24.5 [s, $CH(CH_3)_2$], 24.6 [s, $CH(CH_3)_2$], 28.9 [s, $CH(CH_3)_2$], 49.5 (d, $^1J_{PC}$ = 64.5 Hz), 124.0 (s, imidazolium backbone), 124.6 (s, imidazolium backbone), 125.1 (s, aromatic), 128.3 (d, $^1J_{PC}$ = 19.0 Hz, aromatic), 129.6 (d, J_{PC} = 12.6 Hz, aromatic), 130.1 (s, aromatic), 131.9 (d, J_{PC} = 10.3 Hz, aromatic), 132.4 (s, aromatic), 133.5 (d, J_{PC} = 2.3 Hz, aromatic), 138.3 (s, *ipso* to the imidazole moiety), 145.5 [s, (s, NC(H)N]. ^{31}P-{^{1}H} NMR δ ($CDCl_3$): 36.6 (s, $Ph_2P(O)CH_2$−imidazolium). High-resolution ES$^+$: 443.2242. Calcd for $[C_{28}H_{32}N_2PO]^+$: 443.2247.

The phosphine oxide (2.0 g, 4 mmol) was placed in a three-neck, 1 L flask (tap adapter, double jacket condenser, and a pressure-equalizing dropping funnel) and was dissolved in 110 mL of dried-degassed chlorobenzene by heating to the reflux temperature under a nitrogen atmosphere. The temperature was then maintained at 120 °C, and excess trichlorosilane was added in small potrions (10 mL, 72 mmol, 19-fold excess). After completion of the addition the reaction mixture was heated at 130 °C for 3 h and then cooled to room temperature. After addition of 100 mL of dichloromethane, the excess $SiHCl_3$ was quenched by careful dropwise addition of degassed 10% (w/v) NaOH(aq) at 0 °C. The

(14) Brookhart, M.; Grant, B.; Volpe, A. F. *Organometallics* **1992**, *11*, 3920.

(15) Tsevtkov, E. N.; Tkachenko, S. E.; Yarkevitc, A. N. *Bull. Soc. Chim. Fr.* **1988**, *2*, 339.

(16) Hooft, R. *COLLECT*; Nonius BV: The Netherlands, 1997−2000. Otwinoski, Z.; Minor, W. *SCALEPACK, DENZO. Methods Enzymol.* **1997**, *276*, 307.

organic phase was separated, and the aqueous phase was washed with dichloromethane (3 × 50 mL). The combined organic extracts were dried over $MgSO_4$ and filtered, and the volatiles were removed under reduced pressure. The resulting white solid was washed with ether (2 × 150 mL) and dried under vacuum overnight. The imidazolium salt was further dried azeotropically with toluene and was stored in the glovebox. Yield: 1.0 g (51.6%). ^{1}H NMR δ ($CDCl_3$): 1.03 [6H, d, $^3J_{HH}$ = 6.8 Hz, $CH(CH_3)_2$], 1.15 [6H, d, $^3J_{HH}$ = 6.8 Hz, $CH(CH_3)_2$], 2.01 [2H, septet, $^3J_{HH}$ = 6.8 Hz, $CH(CH_3)_2$], 5.77 (2H, d, $^2J_{PH}$ = 6.4 Hz, Ph_2PCH_2−imidazole), 6.91 (1H, t, $^3J_{HH}$ = 1.7 Hz, aromatic), 7.08 (2H, d, $^3J_{HH}$ = 7.7 Hz, aromatic), 7.31−7.38 (6H, m, aromatic), 7.41 (1H, t, $^3J_{HH}$ = 7.7 Hz, aromatic), 7.51 (1H, t, $^3J_{HH}$ = 1.7 Hz, aromatic), 7.58−7.77 (4H, m, aromatic), 10.5 (1H, t, $^3J_{HH}$ = 1.5 Hz, NCHN). ^{13}C{^{1}H} NMR δ ($CDCl_3$): 23.1 [s, $CH(CH_3)_2$], 23.3 [s, $CH(CH_3)_2$], 27.6 [s, $CH(CH_3)_2$], 47.7 (d, $^1J_{PC}$ = 19.52 Hz, Ph_2PCH_2−imidazolium), 121.44 (d, J_{PC} = 5.1 Hz, aromatic), 122.6 (s, imidazolium, backbone) 123.6 (s, imidazolium backbone), 128.2 (d, J_{PC} = 7.6 Hz, aromatic), 129.1 (s, aromatic), 129.3 (s, aromatic), 130.8 (s, aromatic), 131.6 (d, J_{PC} = 11.5 Hz, aromatic), 132.6 (d, J_{PC} = 20.3 Hz, aromatic), 138.2 (s, *ipso* to the imidazolium moiety), 144.3 [s, NC(H)N]. ^{31}P{^{1}H} NMR: δ ($CDCl_3$): −10.0 (s, Ph_2PCH_2−imidazolium).

(P∧C)Pd(CH_3)$_2$, 1. This was prepared following a previously reported procedure[7] from 0.080 g (0.317 mmol) of Pd(tmeda)Me_2, 0.161 g of [(P∧C)H]$^+$Br$^-$ (1 equiv), and 0.070 g of KN($SiMe_3$)$_2$ (1.1 equiv). Yield: 0.130 g (73%). ^{1}H NMR δ (CD_2Cl_2): −0.53 (3H, d, $^3J_{PH}$ = 8.1 Hz, PdCH_3), −0.32 (3H, d, $^3J_{PH}$ = 8.2 Hz, PdCH_3), 1.06 [6H, d, $^3J_{HH}$ = 6.9 Hz, CH(CH_3)$_2$], 1.23 [6H, d, $^3J_{HH}$ = 6.9 Hz, CH(CH_3)$_2$], 2.55 [2H, sept, $^3J_{HH}$ = 6.9 Hz, CH(CH_3)$_2$], 4.21 [2H, d, $^2J_{PH}$ = 3.3 Hz, (PPh_2CH_2-ylid)PdMe_2], 6.84 (1H, s, ylidene backbone), 7.32 (4H, br d, aromatic), 7.44 (6H, br s, aromatic), 7.62 (4H, m, aromatic). ^{13}C{^{1}H} NMR δ (CD_2Cl_2): −0.4 (d, $^2J_{PC}$ = 18.2 Hz, PdCH_3), 0.2 (d, $^2J_{PC}$ = 19.2 Hz, PdCH_3), 22.4 [s, CH(CH_3)$_2$], 23.7 [s, CH(CH_3)$_2$], 27.5 [s, CH(CH_3)$_2$], 51.9 (d, $^1J_{PC}$ = 24.5 Hz, [PPh_2CH_2-ylid)PdMe_2], 117.9 (s, ylidene backbone), 122.6 (s, ylidene backbone), 123.8 (s, aromatic), 127.8 (d, J_{PC} = 8.85 Hz, aromatic), 128.1 (s, aromatic), 128.3 (s, aromatic), 129.4 (s, aromatic), 131.7 (d, J_{PC} = 26.1 Hz, aromatic), 132.3 (d, J_{PC} = 13.5 Hz, aromatic), 144.9 (s, *ipso* carbon of the aryl group), 190.4 (s, NCN). ^{31}P{^{1}H} NMR δ (CD_2Cl_2): 32.7 [s, (PPh_2CH_2-ylid)PdMe_2]. Anal. Found: C, 63.71; H, 6.38; N, 4.75. Calcd for $C_{30}H_{37}N_2PPd$: C, 63.99; H, 6.62; N, 4.98. X-ray-quality crystals were grown by slow diffusion of petroleum ether into a THF solution of the complex.

(κ^2-C−N)Pd(CH_3)$_2$, 2a. To a solution of 0.080 g (0.317 mmol) of Pd(tmeda)Me_2 in 30 mL of THF at −78 °C was added a precooled solution of 0.135 g (0.443 mmol, 1.4 equiv) of the free carbene in the same solvent (10 mL). The reaction mixture was allowed to reach room temperature slowly overnight. After removal of the volatiles under reduced pressure the pale yellow solid residue was washed with light petroleum (10 mL) and cold ether (−30 °C, 5 mL) to give the product. Yield: 0.050 g (42%). The product deposits Pd black after prolonged exposure to toluene or dichloromethane. ^{1}H NMR δ (CD_2Cl_2): 0.01 (3H, s, PdCH_3), 0.12 (3H, s, PdCH_3), 1.09 (6H, d, $^3J_{HH}$ = 6.9 Hz, CH(CH_3)$_2$), 1.21 (6H, d, $^3J_{HH}$ = 6.9 Hz, CH(CH_3)$_2$), 2.73 (2H, sept, $^3J_{HH}$ = 6.9 Hz, CH(CH_3)$_2$), 6.91 (1H, d, $^3J_{HH}$ = 1.5 Hz, ylidene backbone), 7.22 (2H, distorted ddd, J_{HH} = 5.7, 5.4, and 7.6 Hz, pyridine), 7.31 (2H, d, $^3J_{HH}$ = 7.9 Hz, aromatic), 7.52 (1H, t, $^3J_{HH}$ = 7.9 Hz, aromatic), 7.92 (1H, distorted ddd, J_{HH} = 1, 0.7, and 8.2 Hz, pyridine), 8.06 (1H, d, $^3J_{HH}$ = 1.5 Hz, ylidene backbone), 9.18 (br dt, 1H, pyridine). ^{13}C{^{1}H} NMR δ (CD_2Cl_2): −0.1 (s, PdCH_3), 0.0 (s, PdCH_3), 21.7 (s, CH(CH_3)$_2$), 22.2 (s, CH(CH_3)$_2$), 26.9 (s, CH(CH_3)$_2$), 118.9 (s, ylidene backbone), 120.4 (s, ylidene backbone), 121.4 (s, aromatic), 122.1 (s, aromatic), 123.7 (s, aromatic), 128.3 (s, aromatic), 141.5 (s, aromatic), 143.8 (s, aromatic), 144.1 (s, aromatic), 145.5 (s, aromatic), 147.2 (s, *ipso* carbon of the aryl group). Anal. Found: C, 59.55; H, 6.59; N, 9.31. Calcd for $C_{22}H_{29}N_3Pd$: C, 59.79; H, 6.61; N, 9.51.

(C−N*)Pd(CH_3)$_2$, 2b. This was prepared by a method analogous to **2a** from 0.080 g (0.317 mmol) of Pd(tmeda)Me_2 and 0.101 g (0.317 mmol) of free carbene. Yield: 0.100 mg (81%). ^{1}H NMR δ (CD_2Cl_2): 0.12 (3H, s, PdCH_3), 0.22 (3H, s, PdCH_3), 1.12 (6H, d, $^3J_{HH}$ = 6.9 Hz, CH(CH_3)$_2$), 1.31 (6H, d, $^3J_{HH}$ = 6.9 Hz, CH(CH_3)$_2$), 2.71 (2H, sept, $^3J_{HH}$ = 6.9 Hz, CH(CH_3)$_2$), 2.91 (3H, s, 3-CH_3-pyridine), 6.92 (1H, s, ylidene backbone), 7.31 (3H, m, aromatic), 7.41 (1H, br t, aromatic), 7.72 (1H, br dd, aromatic), 8.07 (1H, d, $^3J_{HH}$ = 2.5 Hz, aromatic), 8.61 (1H, d, $^3J_{HH}$ = 5 Hz, aromatic). ^{13}C{^{1}H} NMR δ(CD_2Cl_2): −0.2 (s, PdCH_3), 0.0 (s, PdCH_3), 19.8 (s, 3-CH_3-pyridine), 21.7 (s, CH(CH_3)$_2$), 22.8 (s, CH(CH_3)$_2$), 26.9 (s, CH(CH_3)$_2$), 115.9 (s, ylidene backbone), 120.4 (s, ylidene backbone), 120.8 (s, aromatic), 122.1 (s, aromatic), 122.5 (s, aromatic), 128.3 (s, aromatic), 141.5 (s, aromatic), 143.8 (s, aromatic), 144.1 (s, aromatic), 144.5 (s, aromatic), 147.2 (s, *ipso* carbon of the aryl group). Anal. Found, C, 60.33; H, 6.56; N, 9.13. Calcd for $C_{23}H_{31}N_3Pd$: C, 60.59; H, 6.85; N, 9.22. Yellow crystals were grown by layering a toluene solution of the complex with light petroleum ether.

(C−N)$_2$Pd(CH_3)$_2$, 3. In the glovebox 80 mg (0.317 mmol) of Pd(tmeda)Me_2 was placed in a Schlenk. A second Schlenk was charged with 194 mg (0.636 mmol) of free carbene. The contents of the two Schlenks were dissolved in dry-degassed THF, and the solution of Pd(tmeda)Me_2 was transferred at room temperature via cannula to the solution of the free carbene. The reaction mixture was stirred overnight, volatiles were removed, and the pale yellow solid was washed with light petroleum ether. The compound is air stable and soluble in dichloromethane, toluene, and ether. Yield: 201 mg (85%). ^{1}H NMR δ (d_8-toluene): −0.11 (6H, s, PdCH_3), 0.82 (6H, d, $^3J_{HH}$ = 6.9 Hz, CH(CH_3)$_2$), 0.98 (6H, d, $^3J_{HH}$ = 6.7 Hz, CH(CH_3)$_2$), 1.09 (6H, d, $^3J_{HH}$ = 6.7 Hz, CH(CH_3)$_2$), 1.42 (6H, d, $^3J_{HH}$ = 6.7 Hz, CH(CH_3)$_2$) 2.62 (2H, sept, $^3J_{HH}$ = 6.7 Hz, CH(CH_3)$_2$), 3.12 (2H, sept, $^3J_{HH}$ = 6.7 Hz, CH(CH_3)$_2$), 6.45 (1H, d, $^3J_{HH}$ = 1.9 Hz, ylidene backbone), 6.51 (1H, d, J_{HH} = 1.6 Hz, aromatic), 6.55 (1H, d, J_{HH} = 1.4 Hz), 6.63 (1H, ddd, J_{HH} = 1.1, 4.9, and 7.1 Hz), 6.83 (2H, t, $^3J_{HH}$ = 7.8 Hz, aromatic) 6.85 (1H, d, $^3J_{HH}$ = 1.9 Hz, ylidene backbone), 6.92 (3H, m, aromatic), 7.03 (1H, br s, aromatic), 7.09 (1H, d, J_{HH} = 1.6 Hz, aromatic), 7.11 (1H, m, aromatic), 8.14 (2H, dd, J_{HH} = 1.1 Hz, 3.8 Hz, aromatic), 8.42 (2H, d, J_{HH} = 2.2 Hz, aromatic), 9.33 (2H, d, J_{HH} = 8.2 Hz, aromatic). ^{13}C{^{1}H} NMR δ (d_8-toluene): −0.4 (s, PdCH_3), 22.1 (s, CH(CH_3)$_2$), 24.1 (s, CH(CH_3)$_2$), 26.5 (s, CH(CH_3)$_2$), 27.3 (s, CH(CH_3)$_2$), 28.6 (s, CH(CH_3)$_2$), 28.8 (s, CH(CH_3)$_2$), 117.1 (s, ylidene backbone), 119.1 (ylidene backbone), 121.3 (s aromatic), 123.8 (s, aromatic), 124.7 (s, aromatic), 125.2 (s, aromatic), 130.7 (s, aromatic), 138 (s, aromatic), 138.9 (s, aromatic), 145.7 (s, aromatic), 147 (s, aromatic), 148.6 (s, aromatic), 152.2 (s, aromatic), 200.1 (s, NCN). Anal. Found: C, 67.61; H, 7.16; N, 11.01. Calcd for $C_{42}H_{52}N_6Pd$: C, 67.50; H, 7.01; N, 11.25. Colorless crystals were grown, by cooling a saturated solution of the compound in toluene to 5 °C.

[(C−N)Pd(methallyl)](BPh_4), 4. A precooled (−78 °C) solution of (C−N) (61 mg, 0.20 mmol) in THF was added to a cold (−78 °C) solution of 40 mg (0.10 mmol) of Pd[(η^3-methallyl)Cl]$_2$ in the same solvent. The mixture was allowed to reach room temperature and stirred for 20 min, and then solid $NaBPh_4$ (68 mg, 0.20 mmol) was added in one portion. After stirring for an additional 15 min the volatiles were removed under reduced pressure and the solid residue was dissolved in CH_2Cl_2 and filtered through Celite. The organic filtrate was evaporated to dryness. Yield: 110 mg (69%). Colorless X-ray-quality crystals were obtained by layering a CH_2Cl_2 solution with light petroleum. ^{1}H NMR δ (CD_2Cl_2): 1.11−1.23 (12H, m, CH(CH_3)$_2$), 1.82 (3H, s, $CH_2CCH_3CH_2$), 2.01−2.41 (4H, br m, CH(CH_3)$_2$ and $CH_2CCH_3CH_2$), 3.25 (1H, s, CH_2CCH_3-

CH*H*), 4.12 (1H, s, CH_2CCH_3CHH), 6.84 (2H, tt, J_{HH} = 1.3 Hz, 8.5 Hz, aromatic), 7.09 (4H, two coinciding d, J_{HH} = 7.4 Hz, 7.5 Hz, aromatic), 7.12 (1H, d, $^3J_{HH}$ = 2.1 Hz, ylidene backbone), 7.35 (12H, br m, aromatic), 7.55 (1H, br t, aromatic), 8.17 (4H, m, aromatic), 8.45 (1H, d, $^3J_{HH}$ = 2.1 Hz, ylidene backbone), 8.51 (1H, ddd, J_{HH} = 0.8 Hz, 1.7 Hz, 5.4 Hz, aromatic). $^{13}C\{^1H\}$ NMR δ (CD_2Cl_2): 22.? (s, $CH(CH_3)_2$), 22.1 (s, $CH(CH_3)_2$), 22.4 (s, $CH_2CCH_3CH_2$), 23.8 (s, $CH(CH_3)_2$), 24.1 (s, $CH(CH_3)_2$), 27.2 (s, $CH(CH_3)_2$), 27.3 (s, $CH(CH_3)_2$), 48.1 (s, $CH_2CCH_3CH_2$), 52.5 (s, $CH_2CCH_3CH_2$), 118.1 (s, ylidene backbone), 119 (ylidene backbone), 121.3 (s aromatic), 123.7 (s, aromatic), 124.8 (s, aromatic), 125.3 (s, aromatic), 125.7 (s, aromatic), 126.3 (br s, aromatic), 127.2 (s, aromatic), 127.9 (s, $CH_2CCH_3CH_2$), 128.8 (s, aromatic), 132.5 (s, aromatic) 138.1 (s, aromatic), 139.2 (s, aromatic), 145.7 (s, aromatic), 146.6 (s, aromatic), 149.4 (s, *ipso* aromatic to aryl group). Anal. Found: C, 73.11; H, 6.19; N, 5.21. Calcd for $C_{48}H_{50}N_3BPd$: C, 73.33; H, 6.41; N, 5.35.

[(C∼P)Pd(methallyl)](BPh$_4$), 5. A precooled solution of the ligand P∧C generated from 212 mg (0.41mmol) of $[(P\wedge C)H]^+Br^-$ and 89 mg (0.45 mmol) of $KN(SiMe_3)_2$ as described above was added to a solution of 80 mg (0.20 mmol) of Pd[(η^3-methallyl)-Cl]$_2$ in THF. After completion of the addition the reaction mixture was allowed to reach room temperature and stirred for 1 h. Addition of solid $NaBPh_4$ (137 mg, 0.40 mmol) was followed by removal of the volatiles under reduced pressure extraction of the residue in CH_2Cl_2, filtration through Celite, and evaporation of the solvents from the organic filtrates. Yield: 90 mg (90%). Colorless X-ray-quality crystals were grown by layering a CH_2Cl_2 solution with ether. ^1H NMR δ (CD_2Cl_2): 0.71−0.89 (12H, m, $CH(CH_3)_2$), 1.35 (3H, s, $CH_2CCH_3CH_2$), 2.28−2.37 (2H, m, $CHHCCH_3CH_2$ and $CH(CH_3)_2$), 2.43 (1H, sept, $^3J_{HH}$ = 6.8 Hz, $CH(CH_3)_2$), 2.91−3.09 (3H, m, $CHHCCH_3CH_2$ and [($PPh_2CH_2CH_2$ylid)Pd(η^3-methallyl)]$^+$), 3.12 and 3.73 (each 1H, br s, $CH_2CCH_3CH_2$), 4.82 (2H, m, [($PPh_2CH_2CH_2$ylid)Pd(η^3-methallyl)]$^+$), 6.91 (1H, s, ylidene backbone), 7.11−7.33 (6H, m, aromatic), 7.35 (5H, br d, aromatic), 7.52 (12H, br s, aromatic), 7.61−7.72 (10H, m, aromatic), 8.17 (1H, s, ylidene backbone). $^{13}C\{^1H\}$ NMR δ (CD_2Cl_2): 21.9 (s, $CH(CH_3)_2$), 22.5 (s, $CH(CH_3)_2$), 22.3 (s, $CH_2CCH_3CH_2$), 23.9 (s, $CH(CH_3)_2$), 24.2 (s, $CH(CH_3)_2$), 26.5 (d, $^1J_{PC}$ = 27.9 Hz, [($PPh_2CH_2CH_2$-ylid)Pd(η^3-methallyl)]Cl), 27.4 (s, $CH(CH_3)_2$), 27.6 (s, $CH(CH_3)_2$), 47.? (s, $CH_2CCH_3CH_2$), 62.5 (d, $^2J_{PC}$ = 9.1 Hz, [($PPh_2CH_2CH_2$-ylid)Pd(η^3-methallyl)]$^+$), 68.4 (d, J_{PC} = 30.3 Hz, $CH_2CCH_3CH_2$), 117.6 (s, ylidene backbone), 122.8 (s, ylidene backbone), 123.1 (s, aromatic), 124.2 (d, J_{PC} = 3.6 Hz, aromatic), 125.8 (s, aromatic), 127.7 (s, $CH_2CCH_3CH_2$), 127.9 (s, aromatic), 128.2 (d, J_{PC} = 11.7 Hz, aromatic), 128.6 (br s., aromatic), 129.9 (s, aromatic), 130.3 (d, J_{PC} = 8.6 Hz), 131.2 (br s, aromatic), 133.2 (s, aromatic), 134.4 (br s, aromatic), 134.9 (s, aromatic), 135.2 (s, aromatic), 149.6 (s, *ipso* aromatic to aryl group). $^{31}P\{^1H\}$ NMR δ (CD_2Cl_2): 22.3 (s, [($PPh_2CH_2CH_2$-ylid)Pd(η^3-methallyl)]$^+$). Anal. Found: C, 74.05; H, 6.28; N, 2.89. Calcd for $C_{57}H_{60}N_2BPPd$: C, 74.31; H, 6.56; N, 3.04.

General Method for the Synthesis of the Cations 6 and 7. Two separate Schleck tubes were charged under N_2 with 1 equiv of the dimethyl complex and the acid $[H(OEt_2)]^+\{B[(3,5\text{-}CF_3)_2C_6H_2]_4\}^-$. The solids were dissolved in CH_2Cl_2, the solutions were cooled to −78 °C, and the acid was added dropwise to the dimethyl complex. Upon addition, the color changed from yellow to almost colorless. The reaction mixture was allowed to warm to −40 °C, when 1.1 equiv of dry-degassed pyridine derivative was added by means of a microsyringe. Then the mixture was allowed to reach room temperature slowly and stirred for 30 min. Removal of the volatiles under reduced pressure and washing of the solid residue with petroleum ether gave the pure cation, which was dried under vacuum.

[(C∧P)Pd(CH$_3$)(Bu^t-py)]$^+$[BAr$^F_4$]$^-$, 6. This was prepared following the general method starting from **1** (55 mg, 0.098 mmol), $H(OEt_2)\{B[(3,5\text{-}CF_3)_2C_6H_2]_4\}$ (92 mg, 1 equiv), and 4-*tert*-butylpyridine (9 μL, 1 equiv). Yield: 110 mg (68%). ^1H NMR δ (CD_2Cl_2): −0.09 (3H, d, $^3J_{PH}$ = 2.6 Hz, PdCH_3), 0.92 (6H, d, $^3J_{HH}$ = 6.8 Hz, $CH(CH_3)_2$), 1.01 (6H, d, $^3J_{HH}$ = 6.8 Hz, $CH(CH_3)_2$), 1.22 (9H, s, 4-*t*Bu-pyridine), 2.30 (2H, sept, $^3J_{HH}$ = 6.7 Hz, $CH(CH_3)_2$), 4.93 (2H, d, $^2J_{PH}$ = 6.6 Hz, [PPh_2CH_2-ylidene]PdMe-(4-tBu-py)$^+$), 7.01 (4H, m, aromatic), 7.33 (2H, m, aromatics), 7.46 (10H, m, aromatics), 7.79 (11H, m, aromatics), 8.01 (2H, d, J_{HH} = 4.5 Hz, aromatics). $^{13}C\{^1H\}$ NMR δ (CD_2Cl_2): 1.9 (s, PdCH_3), 23.2 (s, $CH(CH_3)_2$), 25.1 (s, $CH(CH_3)_2$), 28.6 (s, 4-C$(CH_3)_3$-pyridine), 30.2 (s, $CH(CH_3)_2$), 53.6 (d, $^1J_{PC}$ = 48.9 Hz, [PPh_2CH_2-ylidene]PdMe(4-tBu-py)$^+$), 117.8 (s, ylidene backbone), 122.7 (s, ylidene backbone), 123.1 (s, aromatic), 124.3 (s, aromatic), 126.3 (s, aromatic), 126.8 (br s, aromatic), 128.9 (s, aromatic), 129.2 (s, aromatic), 129.5 (s, aromatic), 129.8 (d, J_{PC} = 15.2 Hz, aromatic), 130.3 (s, aromatic), 130.9 (s, aromatic), 132.8 (s, aromatic), 133.5 (d, J_{PC} = 20.0 Hz, aromatic), 135.2 (s, aromatic), 145.6 (s, aromatic), 150.1 (s, aromatic), 163.1 (q, $^1J_{CF}$ = 49.9 Hz, CF_3 s). $^{31}P\{^1H\}$ NMR δ (CD_2Cl_2): 53.8 (s, [PPh_2CH_2-ylidene]PdMe(4-tBu-py)$^+$). $^{19}F\{^1H\}$ NMR δ (CD_2Cl_2): −63.1 (s, CF_3). Anal. Found: C, 54.25; H, 3.22; N, 2.50. Calcd for $C_{70}H_{55}N_3F_{24}BPPd$: C, 54.51; H, 3.59; N, 2.72.

[(C−N*)Pd(CH$_3$)(py)]$^+$[BAr$^F_4$]$^-$, 7. This was prepared following the general method starting from 0.080 g (0.18 mmol) of **2b**, 0.165 g (1 equiv) of $[H(OEt_2)]^+\{B[(3,5\text{-}CF_3)_2C_6H_2]_4\}^-$, and 15 μL (1.1 equiv) of pyridine. Yield: 0.200 g (82%). ^1H NMR δ (CD_2Cl_2): −0.09 (3H, s, $PdCH_3$), 1.01 (6H, d, $^3J_{HH}$ = 6.9 Hz, $CH(CH_3)_2$), 1.09 (6H, d, $^3J_{HH}$ = 6.9 Hz, $CH(CH_3)_2$), 2.61 (2H, sept, $^3J_{HH}$ = 6.9 Hz, $CH(CH_3)_2$), 2.74 (3H, s, 3-CH_3 pyridine backbone), 7.13 (1H, d, $^3J_{HH}$ = 2.2 Hz, ylidene backbone), 7.20 (1H, m, aromatics), 7.33 (3H, m, aromatics), 7.53 (6H, br s, aromatics), 7.71 (9H, br s, aromatics), 7.86 (1H, dd, J_{HH} = 1.0 Hz, 7.7 Hz, aromatic), 7.91 (1H, br s, aromatic), 8.07 (1H, d, $^3J_{HH}$ = 2.2 Hz, ylidene backbone), 8.54 (2H, dd, J_{HH} = 1.5 Hz, 6.2 Hz, aromatic). $^{13}C\{^1H\}$ NMR δ (CD_2Cl_2): 7.7 (s, $PdCH_3$), 21.5 (s, $CH(CH_3)_2$), 23.8 (s, 3-CH_3 pyridine backbone), 25.2 (s, $CH(CH_3)_2$), 29.4 (s, $CH(CH_3)_2$), 118.2 (s, ylidene backbone), 119.8 (s, ylidene backbone), 121.3 (s, aromatic), 124.0 (s, aromatic), 124.2 (s, aromatic), 124.6 (s, aromatic), 125.0 (s, aromatic), 126.7 (s, aromatic), 127.2 (s, aromatic), 129.8 (q, $^2J_{CF}$ = 30.2 Hz), 131.7 (s, aromatic), 135.1 (s, aromatic), 135.6 (s, aromatic), 139.8 (s, aromatic), 145.5 (s, aromatic), 145.8 (s, aromatic), 146.1 (s, aromatic), 151.8 (s, aromatic), 162.3 (quart, $^1J_{CF}$ = 49.7 Hz, CF_3 s). $^{19}F\{^1H\}$ NMR δ (CD_2Cl_2): −62.8. Anal. Found: C, 51.02; H, 3.12; N, 3.92. Calcd for $C_{59}H_{45}N_4F_{24}BPd$: C, 51.23; H, 3.28; N, 4.05. Colorless crystals of **8** were grown by slow diffusion of petroleum ether in an ether solution.

X-ray Crystallography. A summary of the crystal data, data collection, and refinement for compounds **1**, **2b**, **3**, **4**, **5**, and **7** are given in Table 1.

All data sets were collected on a Enraf-Nonius Kappa CCD area detector diffractometer with an FR591 rotating anode (Mo/Ka radiation) and an Oxford Cryosystems low-temperature device operating in ω scanning mode with ψ and ω scans to fill the Ewald sphere. The programs used for control and integration were Collect, Scalepack, and Denzo.[17] The crystals were mounted on a glass fiber with silicon grease, from Fomblin vacuum oil. All solutions and refinements were performed using the WinGX package[18] and all software packages within. All non-hydrogen atoms were refined using anisotropic thermal parameters, and hydrogens were added using a riding model.

Computational Details. All calculations employed the Gaussian 98 program[18] and used DFT calculations with the BP86 functional throughout. The same approach was used for both models 1 and 2.

(17) Farrugia, L. J. *J. Appl. Crystallogr.* **1999**, *32*, 83.
(18) Frisch M. J.; et al. *Gaussian 98*, Revision A.11.4; Gaussian, Inc.: Pittsburgh, PA, 2001.

Pd and P centers were described using the Stuttgart RECPs and the associated basis sets.[19] For P an extra set of d-orbital polarization functions was added ($\zeta^P = 0.387$).[20] 6-31G** basis sets were used for C, N, and H atoms.[21] For model 1 all stationary points were characterized as minima by computation of the Hessian matrix (all positive eigenvalues). The size of the species in model 2 precluded the routine computation of frequency analyses at the full DFT level, and so for consistency the energies reported in the text do not include zero-point energy corrections. Optimizations were based on the experimental structures of (C∼P)Pd(CH_3)$_2$ and *trans*-P[C∼P)Pd(CH_3)(py)]$^+$. Transition states located with model 2 were, however, fully characterized and show one unique imaginary frequency.

Acknowledgment. We thank Johnson Matthey Catalysts, the University of Southampton, and Heriot-Watt University for financial support (to N.T. and C.S., respectively). We also thank Johnson Matthey Catalysts for a loan of palladium salts.

Supporting Information Available: Full details of the X-ray crystal structures, including complete tables of crystal data, atomic coordinates, bond lengths and angles, and positional and anisotropic thermal parameters. Cartesian coordinates and energies of all computed species. Full ref 18. This material is available free of charge via the Internet at http://pubs.acs.org.

OM0608408

(19) Andrae, D.; Häusserman, U.; Dolg, M.; Stoll, H. Preuss *Theor. Chim. Acta* **1990**, *77*, 123.

(20) Höllwarth, A.; Böhme, M.; Dapprich, S.; Ehlers, A. W.; Gobbi, A.; Jonas, V.; Köhler, K. F.; Stegmann, R.; Veldkamp, A.; Frenking, G. *Chem. Phys. Lett.* **1993**, *208*, 237.

(21) (a) Hehre, W. J.; Ditchfield, R.; Pople, J. A. *J. Chem. Phys.* **1972**, *56*, 2257. (b) Hariharan, P. C.; Pople, J. A. *Theor. Chim. Acta* **1973**, *28*, 213.